Modelling and Analysis of Social Contagion in Dynamic Networks

Alexei Sharpanskykh[1*] and Jan Treur[2]

[1*] Corresponding author: Delft University of Technology, Faculty of Aerospace Engineering
Kluyverweg 1, 2629 HS Delft, The Netherlands
o.a.sharpanskykh@tudelft.nl

[2] VU University Amsterdam, Department of Artificial Intelligence
De Boelelaan 1081, 1081 HV Amsterdam, The Netherlands
treur@few.vu.nl

Abstract. In this paper an agent-based social contagion model with an underlying dynamic network is proposed and analysed. In contrast to the existing social contagion models, the strength of links between agents changes gradually rather than abruptly based on a threshold mechanism. An essential feature of the model – the ability to form clusters – is extensively investigated in the paper analytically and by simulation. Specifically, the distribution of clusters in random and scale-free networks is investigated, the dynamics of links within and between clusters are determined, the minimal distance between two clusters is identified. Moreover, model abstraction methods are proposed by using which aggregated opinion states of clusters of agents can be approximated with a high accuracy. These techniques also improve the computational efficiency of social contagion models (up to 6 times).

Keywords: social contagion models, dynamic networks, agent-based simulation, social decision making

1 Introduction

Social contagion models have been extensively applied to represent and analyse social decision making, opinion formation, spread of diseases and innovation [1, 2, 4, 5, 7, 8, 12, 14]. Such models describe an evolution of states of individual agents under influence of their neighbouring agents by mutual contagion of these states. In many models [4, 9, 16, 17] the links between agents and their neighbors are constant. In some other models [1, 2, 7] such links may disappear abruptly when states of interacting agents are considered to be too different from each other compared to some threshold. Although the behavior of individual agents is usually simple in such models, the global dynamics emerging from many distributed nonlinear interaction between agents are far from trivial. Therefore, to get a better understanding and control of social contagion processes, their dynamics need to be extensively analysed, e.g. by using Complexity Science tools.

In this paper a social contagion model for social decision making with an underlying network of agents with variable link strengths is proposed and analysed. The strength of the links in the model reflects the degree of influence of one agent to another. The higher the influence on an agent, the higher the extent to which information provided by that agent is used in the decision making; sometimes this also is related to the notion of trust (e.g., [6]). In contrast to the existing models [2, 4, 7, 8], the strength of the links changes gradually in a continuous manner, rather than in a discontinuous manner based on a threshold mechanism. Such a mechanism is supported by sociological literature; e.g., [10], in which much evidence exist that relations between individuals develop continuously. The model proposed in this paper covers as special cases a large class of social contagion models considered previously by other authors. Among them are models with constant links between agents (e.g., [4, 9, 17]), as well as models based on a threshold mechanism (e.g., [8]).

Many experimental evidences exist that influence correlates positively with similarity of agents; e.g., [3, 11], either in a static sense or in a dynamic sense. This has led to the principle that the closer the opinions of the interacting agents, the higher the mutual degrees of influence of the agents are (static perspective) or will become (dynamic perspective). Such an assumption underlies most of the existing models of social influence [2, 4, 7, 8, 12, 14].

Inspired by these findings, the dynamics of the links in the proposed model is defined based on the dynamic variant of this principle: closeness of opinions leads to a positive change of connection strength over time. An important feature of the proposed model is that for certain ranges of parameter values clusters of agents emerge that are isolated from each other. A *cluster* is a set of connected agents (i.e., a connected graph) with the same states (e.g., opinions).

The dynamics of social decision making based on the model was analysed by simulation and by mathematical analysis. In particular, the formation and dynamics of clusters of agents was investigated. Both simulation and analytical findings show that the links between the agents within a cluster become stronger over time, and the corresponding degrees of influence tend to 1 (i.e., the highest strength value). At the same time, the strength of the links between the agents in different clusters degrade, and the corresponding degrees of influence tend to 0 (the lowest strength value equivalent to the absence of a connection between the agents). Furthermore, it turns out that different emerging clusters have a certain minimal distance, which was determined analytically. Cluster size distributions in random and scale-free networks were investigated by simulation. The rate of convergence of agent states to equilibrium were investigated both by simulation and analytically and are discussed in the paper. Furthermore, the cluster formation and convergence properties of the proposed model are compared with the corresponding properties of the well-cited threshold-based model developed by Hegselmann and Krause [8].

Although the behavior of individual agents in social contagion models is simple, global dynamics that emerge from interaction of a large number of agents are non-trivial. In this paper abstraction techniques are proposed that allow approximating with a high accuracy aggregated opinion states of clusters of agents emerging in social contagion models with underlying dynamic networks. Furthermore, by model abstraction the computational efficiency of the model can be substantially improved, which is essential for running large-scale agent-based simulations. Specifically, by using model abstraction an approximate form of simulation is obtained, in which clusters of agents are considered as single entities replacing a large number of

interacting agents. The proposed model abstraction procedure allows a 6 times speed up of the simulation of the model described in the paper.

The paper is organized as follows. In Section 2 a social contagion model for social decision making with an underlying dynamic network is proposed. Results of the model analysis analytically and by simulation are presented in Section 3. A model abstraction procedure is proposed and illustrated for this model in Section 4. In Section 5 discussion is provided. Section 6 concludes the paper.

2 The Dynamical Model

The model describes dynamics of decision making by agents in a group as a process of social contagion. The opinion $q_{s,i}$ of an agent i for a decision option s is expressed by a real number in the range $[0, 1]$, reflecting the degree of the agent's support for the option. For each option each agent communicates its opinion to other agents. Agents communicate only with those agents to which they are connected in a social network. In this study two network topologies are considered:

- a *scale-free network topology*: a connected graph with the property that the number of links originating from a given node representing an agent has a power law distribution. In such networks the majority of the agents have one or two links, but a few agents have a large number of links;
- a *random network topology*: a graph, in which links between nodes occur at random. Only connected graphs are considered in this study.

To compare the dynamics in both types of networks, the networks used in this study were generated with 5000 agents and the same average node degree equal to 4.5. This value is close to the average node degree of real social networks.

It is assumed that the agents are able to both communicate and receive opinions to/from the agents, to which they are connected (i.e., the links are bidirectional). Furthermore, a weight $\gamma_{i,j} \in [0,1]$, indicating the degree of influence of agent i on agent j, is associated with each link for each direction of interaction. This weight determines to which extent the opinion of agent i is taken into account in the update of the opinion of agent j for each option. These weights may or may not be symmetric.

It is assumed that the agents interact with each other synchronously, i.e., at the same time (parallel interaction mode). For a quantitative comparison of the dynamics of social contagion models with the parallel interaction mode with models with the sequential interaction mode, please refer to [16, 17].

In the parallel mode, the opinion states of the agents are updated at the same time point t as follows:

$$q_{s,i}(t+\Delta t) = q_{s,i}(t) + \eta_i \, \delta_{s,i}(t)\Delta t \qquad (1)$$

Here η_i is an agent-dependent parameter within the range $[0,1]$, which determines how fast the agent adjusts to the opinion of other agents, and

$$\delta_{s,i}(t) = \sum_{j \in AG} \gamma_{j,i}(t)(q_{s,j}(t) - q_{s,i}(t)) / \sum_{j \in AG} \gamma_{j,i}(t)$$

is the amount of change of the agent i's opinion; AG is the set of all agent names.

The normalization by $\sum_{j \in AG} \gamma_{j,i}(t)$ has the effect that the agent balances by a relative comparison its own self-influence $\gamma_{i,i}(t)$ (i.e., self-assurance that its own opinion is correct) with the influences of other agents.

The degrees of influence $\gamma_{i,j}$ also change over time based on the principle: the closer the opinions of the interacting agents, the higher the mutual degrees of influence of the agents will become. This dynamic principle may be formalised by different functions as follows:

$$\gamma_{i,j}(t+\Delta t) = \gamma_{i,j}(t) + f_{i,j}(\gamma_{i,j}(t), q_{s,i}(t), q_{s,j}(t))\,\Delta t \quad (2)$$

where for function $f_{i,j}(X, Y, Z)$ the main example used is; to make the following exposition clearer, we will substitute the arguments of the function above with the generic variables X, Y and Z:

$$f_{i,j}(X, Y, Z) = \text{Pos}(\alpha_{ij}(\beta_{ij} - (Y-Z)^2))(1-X) - \text{Pos}(-\alpha_{ij}(\beta_{ij} - (Y-Z)^2))X \quad (3)$$

with $\text{Pos}(x) = (|x|+x)/2$, which can be regarded as a parametric version of a Heaviside function; α_{ij} is a speed parameter and β_{ij} is a threshold or tolerance parameter.

Other alternatives for $f_{i,j}(X, Y, Z)$ are:

$$X\,\alpha_{ij}(\beta_{ij} - (Y-Z)^2)(1-X) \qquad X\,\lambda_{ij}(1-|Y-Z|)(1-X) - \zeta_{ij}|Y-Z|$$

Here λ_{ij} is an amplification parameter and ζ_{ij} is an inhibition parameter. Note that (1) and (2) are expressed in difference equation format. In Section 3 they are also considered in differential equation format.

A threshold-based model with abruptly changing links and threshold τ as described in [8] can be obtained by defining $f_{i,j}(X, Y, Z)$ as follows:

$$f_{i,j}(X, Y, Z) = 1-X, \quad \text{when } |Y-Z| \le \tau \quad (4)$$
$$f_{i,j}(X, Y, Z) = -X, \quad \text{when } |Y-Z| > \tau \quad (5)$$

3 Model Analysis

In this section first formal analytical results for the model are presented. After that the model is analysed by simulation.

3.1 Mathematical Analysis

For a mathematical analysis, as a point of departure the following differential equations were derived from (1), (2) and (3) in Section 2. For $\gamma_{i,j}(t)$:

$$\mathbf{d}\gamma_{i,j}(t)/\mathbf{d}t = \text{Pos}(\alpha_{ij}(\beta_{ij} - (q_{s,i}(t) - q_{s,j}(t))^2))(1-\gamma_{i,j}(t)) - \text{Pos}(-\alpha_{ij}(\beta_{ij} - (q_{s,i}(t) - q_{s,j}(t))^2))\,\gamma_{i,j}(t)$$

The differential equations for the $q_{s,i}(t)$ are:

$$\mathbf{d}q_{s,i}(t)/\mathbf{d}t = \eta_i \sum_{j\in AG} \gamma_{j,i}(t)(q_{s,j}(t) - q_{s,i}(t))/\sum_{j\in AG} \gamma_{j,i}(t)$$

Equilibrium values for connection strengths $\gamma_{i,j}(t)$

First, the equilibrium values $\boldsymbol{\gamma}_{i,j}$ for $\gamma_{i,j}(t)$ are addressed. The standard approach is to derive an equilibrium equation from the differential equation by putting $\mathbf{d}\gamma_{i,j}(t)/\mathbf{d}t = 0$. For the specific case for the function $f_{i,j}(X, Y, Z)$ this is

$$\text{Pos}(\alpha_{ij}(\beta_{ij} - (q_{s,i}(t) - q_{s,j}(t))^2))(1-\gamma_{i,j}(t))$$

$$- \text{Pos}(-\alpha_{ij} (\beta_{ij} - (q_{s,i}(t) - q_{s,j}(t))^2)) \gamma_{i,j}(t) = 0$$

The following lemma is used:

Lemma 1

For any numbers α and β the following are equivalent:

(i) $\alpha \text{Pos}(x) + \beta \text{Pos}(-x) = 0$

(ii) $\alpha \text{Pos}(x) = 0$ and $\beta \text{Pos}(-x) = 0$

(iii) $x = 0$ or $x>0$ and $\alpha = 0$ or $x<0$ and $\beta = 0$. ■

Using Lemma 1 it is found that the above equilibrium equation has three solutions

$|\underline{q}_{s,i} - \underline{q}_{s,j}| = \sqrt{\beta_{ij}}$

$|\underline{q}_{s,i} - \underline{q}_{s,j}| > \sqrt{\beta_{ij}}$ and $\gamma_{i,j} = 0$

$|\underline{q}_{s,i} - \underline{q}_{s,j}| < \sqrt{\beta_{ij}}$ and $\gamma_{i,j} = 1$

More can be found about the circumstances under which such equilibria can occur, and for a wider class of functions $f_{i,j}(X, Y, Z)$. The following symmetry properties are relevant.

Definition

The network is called *weakly symmetric* if for all nodes i and j at all time points it holds $\gamma_{i,j} = 0 \Leftrightarrow \gamma_{j,i} = 0$ or, equivalently: $\gamma_{i,j} > 0 \Leftrightarrow \gamma_{j,i} > 0$. The network is called *fully symmetric* if $\gamma_{i,j} = \gamma_{j,i}$ for all nodes i and j at all time points.

Note that the network is fully symmetric if the initial values for $\gamma_{i,j}$ and $\gamma_{j,i}$ are equal and $f_{i,j}(X, Y, Z)=f_{j,i}(X, Z, Y)$ for all X, Y, Z; the latter condition is fulfilled for the specific case if $\alpha_{i,j}=\alpha_{j,i}$ and $\beta_{i,j}=\beta_{j,i}$. The following lemma is used to obtain Theorem 1.

Lemma 2

a) If for some node i at time t for all nodes j with $q_{s,j}(t) > q_{s,i}(t)$ it holds $\gamma_{j,i}(t) = 0$, then $q_{s,i}(t)$ is decreasing at t: $\mathbf{d}q_{s,i}(t)/\mathbf{d}t \leq 0$.

b) If, moreover, a node k exists with $q_{s,k}(t) < q_{s,i}(t)$ and $\gamma_{k,i}(t) > 0$ then $q_{s,i}(t)$ is strictly decreasing at t: $\mathbf{d}q_{s,i}(t)/\mathbf{d}t < 0$.

Proof: a) From the expressions for $\delta_{s,i}(t)$ it follows that $\delta_{s,i}(t) \leq 0$, and therefore $\mathbf{d}q_{s,i}(t)/\mathbf{d}t \leq 0$, so $q_{s,i}(t)$ is decreasing at t.
b) In this case it follows that $\delta_{s,i}(t) < 0$ and therefore $\mathbf{d}q_{s,i}(t)/\mathbf{d}t < 0$, so $q_{s,i}(t)$ is strictly decreasing.■

Theorem 1 (Equilibrium values $\gamma_{i,j}$)

Suppose the network is weakly symmetric, and $f_{i,j}(X,Y,Y) >0$ for all X, Y with $0 < X < 1$. Then in an equilibrium state for any two nodes i and j it holds $\gamma_{i,j} = 0$ or $\gamma_{i,j} = 1$. More specifically, the following hold:

a) In an equilibrium state with $\underline{q}_{s,i} \neq \underline{q}_{s,j}$ it holds $\gamma_{i,j} = 0$.

b) In an equilibrium state with $\underline{q}_{s,i} = \underline{q}_{s,j}$ it holds $\gamma_{i,j} = 0$ or $\gamma_{i,j} = 1$. If $q_{s,i}(t) = q_{s,j}(t)$ and $0 < \gamma_{i,j}(t) < 1$, then $\gamma_{i,j}(t)$ is strictly increasing at time t: $\mathbf{d}\gamma_{i,j}(t)/\mathbf{d}t > 0$.

Proof: a) Suppose in an equilibrium state $\underline{q}_{s,i} \neq \underline{q}_{s,j}$ and $\gamma_{i,j}$, $\gamma_{j,i} > 0$ for some nodes i and j. Take the node i with this property with highest value $\underline{q}_{s,i}$. Then for all nodes j

with $\boldsymbol{\eta}_{s,j} > \boldsymbol{\eta}_{s,i}$ it holds $\boldsymbol{\gamma}_{i,j} = \boldsymbol{\gamma}_{j,i} = 0$. Now apply Lemma 2 to this node i. It follows that $\boldsymbol{d}q_{s,i}(t)/\boldsymbol{d}t < 0$, so $q_{s,i}(t)$ is not in equilibrium. This contradicts the assumption. Therefore $\boldsymbol{\gamma}_{i,j} = 0$ for all nodes i and j with $\boldsymbol{\eta}_{s,i} \neq \boldsymbol{\eta}_{s,j}$.

b) If $0 < \gamma_{i,j}(t) < 1$, then from $q_{s,i}(t) = q_{s,j}(t)$ it follows that $f_{i,j}(\gamma_{i,j}(t), q_{s,i}(t), q_{s,j}(t)) > 0$. From this it follows that $\boldsymbol{d}\gamma_{i,j}(t)/\boldsymbol{d}t > 0$: $\gamma_{i,j}(t)$ is strictly increasing and is not in equilibrium. Therefore in an equilibrium state with $\boldsymbol{\eta}_{s,i} = \boldsymbol{\eta}_{s,j}$ it holds $\boldsymbol{\gamma}_{i,j} = 0$ or $\boldsymbol{\gamma}_{i,j} = 1$.■

Note that the criterion on the function $f_{i,j}(X, Y, Z)$ in Theorem 1 is satisfied for the specific function $f_{i,j}(X, Y, Z) = \text{Pos}(\alpha_{ij} (\beta_{ij} - (Y-Z)^2))(1-X) - \text{Pos}(-\alpha_{ij} (\beta_{ij} - (Y-Z)^2))X$ if and only if $\alpha_{ij}, \beta_{ij} > 0$, which is the case.

Equilibrium values for $q_{s,i}(t)$

In an equilibrium of the network not only the $\gamma_{i,j}$ are in an equilibrium $\boldsymbol{\gamma}_{i,j}$ but also the $q_{s,i}$. From the differential equations for the $q_{s,i}$ it follows that the equilibrium values $\boldsymbol{\eta}_{s,i}$ for $q_{s,i}(t)$ have to satisfy $\sum_{j \in AG} \boldsymbol{\gamma}_{j,i} (\boldsymbol{\eta}_{s,j} - \boldsymbol{\eta}_{s,i}) = 0$.

When $\boldsymbol{\gamma}_{j,i} = 0$ for all j, then from the differential equation it follows that $q_{s,i}$ is in equilibrium irrespective of what value it has. Suppose at least one node j exists with $\boldsymbol{\gamma}_{j,i} \neq 0$. Then the equilibrium equations can be rewritten as

$$\boldsymbol{\eta}_{s,i} = \sum_{j \in AG} (\boldsymbol{\gamma}_{j,i} / \sum_{k \in AG} \boldsymbol{\gamma}_{k,i}) \boldsymbol{\eta}_{s,j}$$

This provides a system of linear equations for the $\boldsymbol{\eta}_{s,i}$ that could be solved, unless they are trivial or dependent. To analyse this, suppose S_i is the cluster (of size s_i) of nodes with same equilibrium value as $\boldsymbol{\eta}_{s,i}$:

$$S_i = \{ j \mid \boldsymbol{\eta}_{s,j} = \boldsymbol{\eta}_{s,i} \} \qquad s_i = \#(S_i)$$

In Theorem 1a) above it has been found that $\boldsymbol{\gamma}_{j,i} = 0$ if $j \notin S_i$. Therefore

$$\sum_{j \in AG} \boldsymbol{\gamma}_{j,i} \boldsymbol{\eta}_{s,j} = \sum_{j \in S_i} \boldsymbol{\gamma}_{j,i} \boldsymbol{\eta}_{s,j} = \sum_{j \in S_i} \boldsymbol{\gamma}_{j,i} \boldsymbol{\eta}_{s,i}$$

Then the equilibrium equation for $\boldsymbol{\eta}_{s,i}$ becomes:

$$\boldsymbol{\eta}_{s,i} = \sum_{j \in AG} \boldsymbol{\gamma}_{j,i} \boldsymbol{\eta}_{s,j} / \sum_{j \in AG} \boldsymbol{\gamma}_{j,i} = \sum_{j \in S_i} \boldsymbol{\gamma}_{j,i} \boldsymbol{\eta}_{s,j} / \sum_{j \in S_i} \boldsymbol{\gamma}_{j,i} = \boldsymbol{\eta}_{s,i}$$

Thus these equations do not provide a feasible way to obtain information about the equilibrium values $\boldsymbol{\eta}_{s,i}$. However, by different methods at least some properties of the equilibrium values $\boldsymbol{\eta}_{s,i}$ can be derived, as is shown below.

The following conditions on the function $f_{i,j}(X, Y, Z)$ are assumed:

Definition

The function $f_{i,j}(X, Y, Z)$ has a *threshold* τ for $Y - Z$ if

a) For all Y and Z *it holds*

$$f_{i,j}(0, Y, Z) \geq 0 \qquad f_{i,j}(1, Y, Z) \leq 0$$

b) For all X with $0 < X < 1$ and all Y and Z it holds

$$f_{i,j}(X, Y, Z) > 0 \quad \text{iff} \quad |Y - Z| < \tau$$
$$f_{i,j}(X, Y, Z) = 0 \quad \text{iff} \quad |Y - Z| = \tau$$
$$f_{i,j}(X, Y, Z) < 0 \quad \text{iff} \quad |Y - Z| > \tau$$

Note that (given that $\alpha_{ij} > 0$ is assumed) the function

$f_{i,j}(X, Y, Z) = \text{Pos}(\alpha_{ij}(\beta_{ij} - (Y-Z)^2))(1-X) - \text{Pos}(-\alpha_{ij}(\beta_{ij} - (Y-Z)^2))X$
satisfies these conditions for threshold $\sqrt{\beta_{ij}}$.

Theorem 2 (Distance between equilibrium values $\underline{\boldsymbol{q}}_{s,i}$)
Suppose the network is weakly symmetric, the function $f_{i,j}(X, Y, Z)$ has a threshold τ, and the network reaches an equilibrium state with values $\underline{\boldsymbol{q}}_{s,i}$ for the different nodes i. Then for every two nodes i and j if their equilibrium values $\underline{\boldsymbol{q}}_{s,i}$ and $\underline{\boldsymbol{q}}_{s,j}$ are distinct, and the initial values for $\gamma_{i,j}$ and $\gamma_{j,i}$ are nonzero, they have a distance of at least τ: $|\underline{\boldsymbol{q}}_{s,i} - \underline{\boldsymbol{q}}_{s,j}| \geq \tau$. In particular, when all initial values for $\gamma_{i,j}$ and $\gamma_{j,i}$ are nonzero, there are at most $1 + 1/\tau$ distinct equilibrium values $\underline{\boldsymbol{q}}_{s,i}$.

Proof: Suppose two nodes are given with distinct equilibrium values $\underline{\boldsymbol{q}}_{s,i}$ and $\underline{\boldsymbol{q}}_{s,j}$ with distance less than τ. Then $|\underline{\boldsymbol{q}}_{s,i} - \underline{\boldsymbol{q}}_{s,j}| = \tau - \delta$ for some $\delta > 0$. Without loss of generality it can be assumed that $\underline{\boldsymbol{q}}_{s,j} < \underline{\boldsymbol{q}}_{s,i}$. Because $q_{s,i}(t)$ converges to $\underline{\boldsymbol{q}}_{s,i}$ and $q_{s,j}(t)$ converges to $\underline{\boldsymbol{q}}_{s,j}$ it follows that there exists a t such that for all t' with $t' \geq t$ it holds

$$|q_{s,i}(t') - \underline{\boldsymbol{q}}_{s,i}| < \tfrac{1}{2}\delta \quad \text{and} \quad |q_{s,j}(t') - \underline{\boldsymbol{q}}_{s,i}| < \tfrac{1}{2}\delta$$

Therefore for all $t' \geq t$ it holds (by the triangle inequality)

$$\begin{aligned} |q_{s,i}(t') - q_{s,j}(t')| &= |(q_{s,i}(t') - \underline{\boldsymbol{q}}_{s,i}) - (q_{s,j}(t') - \underline{\boldsymbol{q}}_{s,j}) + (\underline{\boldsymbol{q}}_{s,i} - \underline{\boldsymbol{q}}_{s,j})| \\ &\leq |q_{s,i}(t') - \underline{\boldsymbol{q}}_{s,i}| + |q_{s,j}(t') - \underline{\boldsymbol{q}}_{s,j}| + |\underline{\boldsymbol{q}}_{s,i} - \underline{\boldsymbol{q}}_{s,j}| \\ &< \tfrac{1}{2}\delta + \tfrac{1}{2}\delta + \tau - \delta = \tau \end{aligned}$$

So, $|q_{s,i}(t') - q_{s,j}(t')| < \tau$ for all $t' \geq t$.

Since the function $f_{i,j}(X, Y, Z)$ has threshold τ, from this it follows that for all $t' \geq t$ when $0 < \gamma_{i,j}(t') < 1$ it holds

$$f_{i,j}(\gamma_{i,j}(t'), q_{s,i}(t'), q_{s,j}(t')) > 0$$

From the differential equation for $\gamma_{i,j}(t)$ it follows that when $0 < \gamma_{i,j}(t') < 1$ it holds that $\boldsymbol{d}\gamma_{i,j}(t')/\boldsymbol{d}t > 0$ for all $t' \geq t$. From Theorem 1a) it follows that the equilibrium value for $\gamma_{i,j}(t)$ is $\boldsymbol{\gamma}_{i,j} = 0$. Taking into account that always $\gamma_{i,j}(t') \geq 0$, and that $\boldsymbol{d}\gamma_{i,j}(t')/\boldsymbol{d}t > 0$ when $0 < \gamma_{i,j}(t') < 1$ for all $t' \geq t$ this equilibrium value $\boldsymbol{\gamma}_{i,j} = 0$ can only be reached when $\gamma_{i,j}(t) = 0$ for all t, which contradicts the fact that the initial value for $\gamma_{i,j}$ is nonzero. Summarising, the assumption that $|\underline{\boldsymbol{q}}_{s,i} - \underline{\boldsymbol{q}}_{s,j}| < \tau$ has been falsified, so the distance between two distinct equilibrium values $\underline{\boldsymbol{q}}_{s,i}$ and $\underline{\boldsymbol{q}}_{s,j}$ is at least τ: $|\underline{\boldsymbol{q}}_{s,i} - \underline{\boldsymbol{q}}_{s,j}| \geq \tau$. The last statement of the theorem follows since the interval $[0, 1]$ can be divided in at most $1/\tau$ subintervals of length τ. ■

In case the network is fully symmetric (i.e., $\gamma_{j,i} = \gamma_{i,j}$ for all i and j) the equilibrium values $\underline{\boldsymbol{q}}_{s,i}$ can be related to the initial values $q_{s,i}(t)$. In this case the sum $\Sigma_i q_{s,i}(t)$ is preserved: $\Sigma_{i \in AG} q_{s,i}(t) = \Sigma_{i \in AG} q_{s,i}(t')$ for all t and t'. From $\gamma_{j,i} = \gamma_{i,j}$ this can be established as follows:

$$\begin{aligned} \boldsymbol{d}\,\Sigma_{i \in AG}\, q_{s,i}(t)/\boldsymbol{d}t &= \Sigma_{i \in AG}\, \boldsymbol{d}\, q_{s,i}(t)/\boldsymbol{d}t = \eta_i \Sigma_{i \in AG} \Sigma_{j \in AG} \gamma_{j,i}(t)(q_{s,j}(t) - q_{s,i}(t))/\Sigma_{j \in AG} \gamma_{j,i}(t) \\ &= \eta_i [\Sigma_{k \in AG} \Sigma_{i \in AG} \gamma_{i,k} q_{s,k}(t) - \Sigma_{k \in AG} \Sigma_{i \in AG} \gamma_{i,k}\, q_{s,k}(t)]/\Sigma_{j \in AG} \gamma_{j,i}(t) = 0 \end{aligned}$$

The fact that $\Sigma_{i \in AG} q_{s,i}(t)$ is preserved can be applied to compare the equilibrium values $\underline{\boldsymbol{q}}_{s,i}$ to the initial values $q_{s,i}(t_0)$. Let $\underline{\boldsymbol{S}}$ be the set of clusters of equilibria:

$$\underline{\boldsymbol{S}} = \{S_i \mid i \text{ any node}\}$$

For $C \in \underline{S}$ define

$\underline{\boldsymbol{q}}_{s,C} = \underline{\boldsymbol{q}}_{s,j}$ for any $j \in C$

$s_C = \#(C) = s_j$ for any $j \in C$

Then from the preservation it follows

$\Sigma_{i \in AG} \underline{\boldsymbol{q}}_{s,i} = \Sigma_{i \in AG} q_{s,i}(t_0)$

Therefore

$\Sigma_{C \in \underline{S}} \Sigma_{i \in C} \underline{\boldsymbol{q}}_{s,i} = \Sigma_{i \in AG} q_{s,i}(t_0)$

$\Sigma_{C \in \underline{S}} (s_C/n) \underline{\boldsymbol{q}}_{s,C} = \Sigma_{i \in AG} q_{s,i}(t_0)/n$

with $n=\#(AG)$ the total number of nodes. So, the weighted average over the clusters (with as weights the fraction of the total number of nodes in the cluster) is the average of the initial values $q_{s,i}(t_0)$. These are summarised in the following theorem:

Theorem 3 (Equilibria $\underline{\boldsymbol{q}}_{s,i}$ in fully symmetric case)

Suppose the network is fully symmetric. Then the sum $\Sigma_{i \in AG} q_{s,i}(t)$ is preserved over time. Moreover, the weighted average of the equilibrium values for the clusters, with the fraction of the total number of nodes in the cluster as weights, is the average of the initial values:

$\Sigma_{C \in \underline{S}} (s_C/n) \underline{\boldsymbol{q}}_{s,C} = \Sigma_{i \in AG} q_{s,i}(t_0)/n$ ■

Analysis of behaviour around equilibria

Next it is analysed whether equilibria are attracting and how fast they are approached. This analysis corresponds to a classical linear stability analysis found in dynamical systems theory. In short, we examine the stability of the dynamics in terms of Lyapunov exponents associated with the linearised flow around equilibria. Again, suppose $\underline{\boldsymbol{\gamma}}_{i,j}$ are equilibrium values for $\gamma_{i,j}(t)$, and $\underline{\boldsymbol{q}}_{s,i}$ for $q_{s,i}(t)$. The equilibrium criteria ensure that $f_{i,j}(\underline{\boldsymbol{\gamma}}_{i,j}, \underline{\boldsymbol{q}}_{s,i}, \underline{\boldsymbol{q}}_{s,j}) = 0$ and $\Sigma_{j \neq i} \underline{\boldsymbol{\gamma}}_{j,i} (\underline{\boldsymbol{q}}_{s,j} - \underline{\boldsymbol{q}}_{s,i}) = 0$. For convergence speed the following definition is used:

Definition

If a variable $y(t)$ converges to $\underline{\boldsymbol{y}}$ over time t the *convergence speed* is

$cs = - \boldsymbol{d}(\underline{\boldsymbol{y}} - y(t))/\boldsymbol{d}t \; / \; (\underline{\boldsymbol{y}} - y(t))$

The *asymptotic convergence speed* is the limit of this for $t \to \infty$. Note that for a process with exponential convergence according to a function

$\underline{\boldsymbol{y}} - y(t) = (\underline{\boldsymbol{y}} - y(t_0)) \, e^{-\alpha(t-t_0)}$

the convergence speed is α. For exponential convergence sometimes also *a half-value time* is used as a measure for convergence. In this case that would be $\log(2)/\alpha$.

Often in processes the variables have such an asymptotic exponential character, which can be found by determining a first order approximation. Therefore a standard approach to analyse the behaviour close to equilibria is by determining a linear approximation. To this end, write

$\gamma_{i,j}(t) = \underline{\boldsymbol{\gamma}}_{i,j} + \nu_{i,j}(t)$

$q_{s,i}(t) = \underline{\boldsymbol{q}}_{s,i} + \rho_{s,i}(t)$

For an attracting equilibrium $\nu_{i,j}(t)$ and $\rho_{s,i}(t)$ converge to 0.

Asymptotic convergence speed for $\gamma_{i,j}(t)$

First the behaviour near equilibria for the connection strengths $\gamma_{i,j}$ are addressed. By substituting the above expressions for $q_{s,i}(t)$ and $\gamma_{i,j}(t)$ in the differential equation for $\gamma_{i,j}(t)$ the following first order approximation can easily be derived:

$$\begin{aligned}
&\mathbf{d}\nu_{i,j}(t)/\mathbf{d}t = f_{i,j}(\boldsymbol{\gamma}_{i,j} + \nu_{i,j}(t), \boldsymbol{q}_{s,i} + \rho_{s,i}(t), \boldsymbol{q}_{s,j} + \rho_{s,j}(t)) \\
&= f_{i,j}(\boldsymbol{\gamma}_{i,j}, \boldsymbol{q}_{s,i}, \boldsymbol{q}_{s,j}) + \partial f_{i,j}/\partial X(\boldsymbol{\gamma}_{i,j}, \boldsymbol{q}_{s,i}, \boldsymbol{q}_{s,j})\ \nu_{i,j}(t) + \\
&\quad \partial f_{i,j}/\partial Y(\boldsymbol{\gamma}_{i,j}, \boldsymbol{q}_{s,i}, \boldsymbol{q}_{s,j})\ \rho_{s,i}(t) + \partial f_{i,j}/\partial Z(\boldsymbol{\gamma}_{i,j}, \boldsymbol{q}_{s,i}, \boldsymbol{q}_{s,j})\ \rho_{s,j}(t)) \\
&= \partial f_{i,j}/\partial X(\boldsymbol{\gamma}_{i,j}, \boldsymbol{q}_{s,i}, \boldsymbol{q}_{s,j})\ \nu_{i,j}(t) + \\
&\quad \partial f_{i,j}/\partial Y(\boldsymbol{\gamma}_{i,j}, \boldsymbol{q}_{s,i}, \boldsymbol{q}_{s,j})\ \rho_{s,i}(t) + \partial f_{i,j}/\partial Z(\boldsymbol{\gamma}_{i,j}, \boldsymbol{q}_{s,i}, \boldsymbol{q}_{s,j})\ \rho_{s,j}(t))
\end{aligned}$$

For the specific function $f_{i,j}(X, Y, Z) = X\ \alpha_{ij}\ (\beta_{ij} - (Y-Z)^2)(1-X)$ the following partial derivatives can be found:

$$\begin{aligned}
&\partial f_{i,j}/\partial X = (1 - 2X)\ \alpha_{ij}\ (\beta_{ij} - (Y-Z)^2) \\
&\partial f_{i,j}/\partial Y = -2X\ \alpha_{ij}\ (Y-Z)(1-X) \\
&\partial f_{i,j}/\partial Z = 2X\ \alpha_{ij}\ (Y-Z)(1-X)
\end{aligned}$$

From Theorem 1 it follows that $\boldsymbol{\gamma}_{i,j} = 0$ or $\boldsymbol{\gamma}_{i,j} = 1$, so:

$$\partial f_{i,j}/\partial Y(\boldsymbol{\gamma}_{i,j}, \boldsymbol{q}_{s,i}, \boldsymbol{q}_{s,j}) = \partial f_{i,j}/\partial Z(\boldsymbol{\gamma}_{i,j}, \boldsymbol{q}_{s,i}\ \boldsymbol{q}_{s,j}) = 0$$

Therefore

$$\begin{aligned}
\mathbf{d}\nu_{i,j}(t)/\mathbf{d}t &= \partial f_{i,j}/\partial X(\boldsymbol{\gamma}_{i,j}, \boldsymbol{q}_{s,i}, \boldsymbol{q}_{s,j})\ \nu_{i,j}(t) \\
&= (1 - 2\boldsymbol{\gamma}_{i,j})\ \alpha_{ij}\ (\beta_{ij} - (\boldsymbol{q}_{s,i} - \boldsymbol{q}_{s,j})^2)\ \nu_{i,j}(t)
\end{aligned}$$

This is a simple first-order linear differential equation in $\nu_{i,j}(t)$ with explicit solution

$$\nu_{i,j}(t) = \nu_{i,j}(t_0)\ e^{-\mu_{ij}(t - t_0)}$$

where $\mu_{ij} = (1 - 2\boldsymbol{\gamma}_{i,j})\ \alpha_{ij}\ ((\boldsymbol{q}_{s,i} - \boldsymbol{q}_{s,j})^2 - \beta_{ij})$ is the asymptotic convergence speed. For the case that $\boldsymbol{q}_{s,i} \neq \boldsymbol{q}_{s,j}$ from Theorem 1a) it follows that $\boldsymbol{\gamma}_{i,j} = 0$, and from Theorem 2 that $|\boldsymbol{q}_{s,i} - \boldsymbol{q}_{s,j}| \geq \sqrt{\beta_{ij}}$. Then the above formula for the asymptotic convergence speed simplifies to:

$$\begin{aligned}
&\mu_{ij} = \alpha_{ij}\ ((\boldsymbol{q}_{s,i} - \boldsymbol{q}_{s,j})^2 - \beta_{ij}) \geq 0 \\
&\nu_{i,j}(t) = \nu_{i,j}(t_0)\ e^{-\alpha_{ij}\ ((\boldsymbol{q}_{s,i} - \boldsymbol{q}_{s,j})^2 - \beta_{ij})(t - t_0)}
\end{aligned}$$

For this case when $|\boldsymbol{q}_{s,i} - \boldsymbol{q}_{s,j}| > \sqrt{\beta_{ij}}$ the asymptotic convergence speed is

$$\mu_{ij} = \alpha_{ij}\ ((\boldsymbol{q}_{s,i} - \boldsymbol{q}_{s,j})^2 - \beta_{ij}) > 0$$

Since this is positive the equilibrium is attracting. The speed is dependent on $\boldsymbol{q}_{s,j}$ and $\boldsymbol{q}_{s,i}$: it is quadratic in the distance $|\boldsymbol{q}_{s,i} - \boldsymbol{q}_{s,j}|$. For the other case, consider $\boldsymbol{q}_{s,j} = \boldsymbol{q}_{s,i}$ (see Theorem 1b)). It now follows that the asymptotic convergence speed is $\mu_{ij} = -(1 - 2\boldsymbol{\gamma}_{i,j})\ \alpha_{ij}\beta_{ij}$ which is independent of $\boldsymbol{q}_{s,i}$. For $\boldsymbol{\gamma}_{i,j} = 0$ this is $-\alpha_{ij}\beta_{ij}$ which is negative, and therefore this equilibrium is not attracting. For $\boldsymbol{\gamma}_{i,j} = 1$ it holds $\mu_{ij} = \alpha_{ij}\beta_{ij}$ which is positive, so in this case the equilibrium is attracting with asymptotic convergence speed $\alpha_{ij}\beta_{ij}$, according to $\nu_{i,j}(t) = \nu_{i,j}(t_0)\ e^{-\alpha_{ij}\beta_{ij}(t - t_0)}$

These results are summarised in the following theorem.

Theorem 4 (Asymptotic convergence of connection strengths)
Suppose the network is weakly symmetric and $f_{i,j}(X, Y, Z) = X\ \alpha_{ij}\ (\beta_{ij} - (Y-Z)^2)(1-X)$. Consider an equilibrium state with values $\underline{q}_{s,i}$ for the node states $q_{s,i}(t)$ and $\gamma_{i,j}$ for the connections $\gamma_{i,j}(t)$. Then the following hold:
a) If $|\underline{q}_{s,i} - \underline{q}_{s,j}| > \sqrt{\beta_{ij}}$ then the equilibrium $\gamma_{i,j} = 0$ is attracting with asymptotic convergence speed $\alpha_{ij}\ ((\underline{q}_{s,i} - \underline{q}_{s,j})^2 - \beta_{ij})$.
b) If $\underline{q}_{s,i} = \underline{q}_{s,j}$ then only the equilibrium $\gamma_{i,j} = 1$ is attracting with asymptotic convergence speed $\alpha_{ij}\beta_{ij}$.

Note that for nodes i and j for which $|\underline{q}_{s,i} - \underline{q}_{s,j}|$ is very close to $\sqrt{\beta_{ij}}$, the asymptotic convergence speed is very close to 0. A special case occurs when $|\underline{q}_{s,i} - \underline{q}_{s,j}| = \sqrt{\beta_{ij}}$. Then the first-order approximation for $d\nu_{i,j}(t)/dt$ made above becomes 0; in this case second-order terms (which above have been neglected) have to be considered, making the analysis a more complex. Interestingly, these second order generally lead to critical behaviour in coupled dynamical systems - which itself is the focus of much attention in the study of self-organised systems.

Asymptotic convergence speed for $q_{s,i}(t)$
Next the asymptotic convergence speed for reaching equilibrium values $\underline{q}_{s,i}$ by $q_{s,i}(t)$ is addressed. This time the expressions for $q_{s,i}(t)$ and $\gamma_{j,i}(t)$ are substituted in the differential equations for the $q_{s,i}(t)$, thereby neglecting second-order terms:

$$
\begin{aligned}
&d\rho_{s,i}(t)/dt = \\
&\eta_i \textstyle\sum_{j\neq i} (\gamma_{j,i} + \nu_{j,i}(t))((\underline{q}_{s,j} + \rho_{s,j}(t)) - (\underline{q}_{s,i} + \rho_{s,i}(t))) \\
&= \eta_i \textstyle\sum_{j\neq i} (\gamma_{j,i} + \nu_{j,i}(t))((\underline{q}_{s,j} - \underline{q}_{s,i}) + (\rho_{s,j}(t) - \rho_{s,i}(t))) \\
&= \eta_i \textstyle\sum_{j\neq i} [\gamma_{j,i} ((\underline{q}_{s,j} - \underline{q}_{s,i}) + (\rho_{s,j}(t) - \rho_{s,i}(t)) + \nu_{j,i}(t)(\underline{q}_{s,j} - \underline{q}_{s,i})] \\
&= \eta_i \textstyle\sum_{j\neq i} [\gamma_{j,i} (\rho_{s,j}(t) - \rho_{s,i}(t)) + \nu_{j,i}(t)(\underline{q}_{s,j} - \underline{q}_{s,i})]
\end{aligned}
$$

Recall

$$S_i = \{\ j \mid \underline{q}_{s,j} = \underline{q}_{s,i}\ \} \qquad s_i = \#(S_i)$$

The sum for $j \neq i$ above can be split in two parts:
- a part for which $\underline{q}_{s,j} = \underline{q}_{s,i}$ (j in cluster S_i), and $\gamma_{j,i} = 1$
- a part for which $\underline{q}_{s,j} \neq \underline{q}_{s,i}$ (j not in cluster S_i), and $\gamma_{j,i} = 0$

This results in:

$$
\begin{aligned}
d\rho_{s,i}(t)/dt &= \eta_i\ [\textstyle\sum_{j\neq i, j\in S_i} (\rho_{s,j}(t) - \rho_{s,i}(t)) + \sum_{j\notin S_i} (\underline{q}_{s,j} - \underline{q}_{s,i})\nu_{j,i}(t)] \\
&= \eta_i\ [\textstyle\sum_{j\in S_i} (\rho_{s,j}(t) - \rho_{s,i}(t)) + \sum_{j\notin S_i} (\underline{q}_{s,j} - \underline{q}_{s,i})\nu_{j,i}(t)]
\end{aligned}
$$

So, as an approximation an inhomogeneous system of linear first-order differential equations for the $\rho_{s,i}(t)$ is obtained, which in principle is analytically solvable by explicit expressions. Here for $\nu_{j,i}(t)$, as above it is assumed that it converges to 0 according to an expression

$$\nu_{j,i}(t) = \nu_{j,i}(t_0)\ e^{-\mu_{ji}(t-t_o)}$$

for some asymptotic convergence speed $\mu_{j,i} > 0$. As an example, for the specific function $f_{j,i}(X, Y, Z)$ considered above it holds:

$$\mu_{j,i} = \alpha_{j,i} ((\underline{\boldsymbol{q}}_{s,j} - \underline{\boldsymbol{q}}_{s,i})^2 - \beta_{j,i})$$

Note that, when $\alpha_{j,i}$ and $\beta_{j,i}$ are assumed uniform (independent of i and j), then $\mu_{j,i}$ monotonically depends on $|\underline{\boldsymbol{q}}_{s,j} - \underline{\boldsymbol{q}}_{s,i}|$. In particular, the lowest $\mu_{j,i}$ (lowest asymptotic convergence speed) occurs for the lowest distance $|\underline{\boldsymbol{q}}_{s,j} - \underline{\boldsymbol{q}}_{s,i}|$ for $\underline{\boldsymbol{q}}_{s,j} \neq \underline{\boldsymbol{q}}_{s,i}$ among the equilibrium values for $q_{s,i}(t)$.

However, the approximate analysis discussed here applies to a more general function $f_{j,i}(X, Y, Z)$. To obtain a feasible analysis, the assumption is made that the asymptotic convergence speed of the $\gamma_{j,i}(t)$ is higher than the asymptotic convergence speed of the $q_{s,i}(t)$. Then from the equations above the sum with the $\nu_{j,i}(t)$ can be neglected, thus obtaining

$$d\rho_{s,i}(t)/dt = \eta_i \sum_{j \in S_i} (\rho_{s,j}(t) - \rho_{s,i}(t))$$

The explicit solutions for these differential equations for the $\rho_{s,i}(t)$ have the form of linear combinations of exponential functions $e^{-\lambda i(t-t_0)}$ for some λ_i. Moreover, given that in an equilibrium that is attracting the $\rho_{s,i}(t)$ converge to 0, these λ_i will be positive, and the asymptotic convergence speed depends on the dominant term based on the smallest of the λ_i. Based on this dominance the following approximations can be obtained using the smallest λ_i:

$$\rho_{s,i}(t) = \rho_{s,i}(t_0)\, e^{-\lambda i(t-t_0)}$$

The results are summarised in the following theorem:

Theorem 5 (Asymptotic convergence of the $q_{s,i}(t)$)
When the asymptotic convergence speed of $q_{s,i}(t)$ is lower than the lowest asymptotic convergence speed of the $\gamma_{j,i}(t)$, then the following hold:

a) For a node i with lowest asymptotic speed λ_i in S_i:

$$\lambda_i = \eta_i [s_i - m_i (\sum_{j \in m S_i} q_{s,j}(t_0) / m_i - \underline{\boldsymbol{q}}_{s,i}) / (q_{s,i}(t_0) - \underline{\boldsymbol{q}}_{s,i})]$$

When all nodes in S_i have the same asymptotic convergence speed λ_i, then:

$$\lambda_i = \eta_i s_i [1 - (\sum_{j \in S_i} q_{s,j}(t_0) / s_i - \underline{\boldsymbol{q}}_{s,i}) / (q_{s,i}(t_0) - \underline{\boldsymbol{q}}_{s,i})]$$

When there is only one node i with lowest asymptotic convergence speed λ_i in S_i, then

$$\lambda_i = \eta_i (s_i - 1)$$

b) When a node i exists which has not lowest asymptotic convergence speed in S_i, then

$$\underline{\boldsymbol{q}}_{s,i} = \sum_{j \in m S_i} q_{s,j}(t_0) / m_i.$$

3.2 Analysis by Simulation

In this section two model variants from Section 2 are analysed by simulation: model *M1* with continuously changing links (equation (3)) and threshold-based model *M2* with abruptly changing links (equations (4) and (5)). Both models have the same threshold $\tau = \sqrt{\beta_{ij}}$. The models were simulated in Matlab.

To compare the models, 10 different random network topologies with 5000 agents and 10 different scale-free network topologies with 5000 agents were generated. The scale-free networks were obtained using the Complex Networks Package [13] with scale-free degree distribution of α=-2.2 (as in many real social networks). The average node degree of such networks with 5000 agents equals 4.5. The random networks were generated with the same average node dergree. The agents formed opinions on some topic *s*. The parameters of the agents and of the links were uniformly distributed as follows: $\eta_i \in [0.5, 1]$; $q_{s,i}(0) \in [0,1]$; $\gamma_{i,j}(0) \in (0, 1]$ (in model *M2* $\gamma_{i,j}(0)$=1, if there was a link between *i* and *j,* and *0* otherwise). These distributions are assumed to represent the diversity that naturally occurs in real-world agent populations.

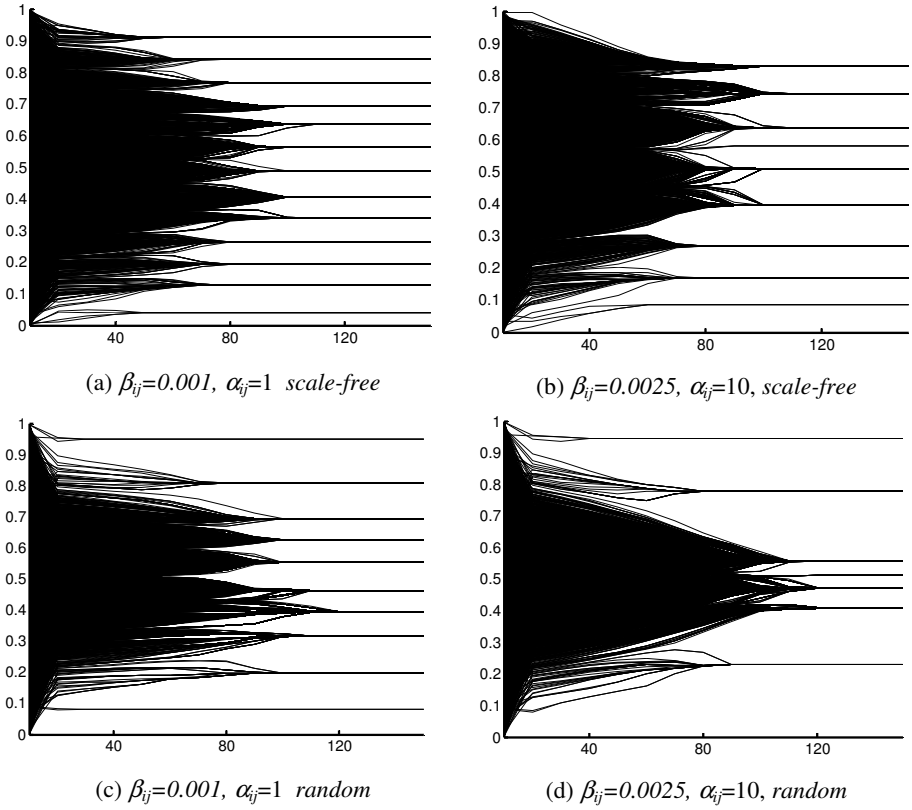

(a) β_{ij}=0.001, α_{ij}=1 *scale-free*

(b) β_{ij}=0.0025, α_{ij}=10, *scale-free*

(c) β_{ij}=0.001, α_{ij}=1 *random*

(d) β_{ij}=0.0025, α_{ij}=10, *random*

Fig. 1. The change of the opinions $q_{s,i}(t)$ in the model with 100 agents with scale free and random networks. The horizontal axis is time (s) and the vertical axis is the degree of support for option *s.* In both types of networks clusters of agents emerge, which stabilize over time to equilibrium values. Generally, more clusters emerge in the scale-free networks than in the random networks with the same α_{ij} and β_{ij} parameter settings. Furthermore, the higher the value of β_{ij} the less clusters emerge in both model types. Besides β_{ij}, parameter α_{ij} also influences the number of clusters with the limit $1 + 1/\sqrt{\beta_{ij}}$, however in a more intricate manner. For example, in the random networks the largest number of clusters emerges when α_{ij} takes intermediate values (around 10), whereas in the scale-free networks many clusters tend to form with low values of α_{ij}.

The simulation time was 300 time points and $\Delta t=1$.

In the previous section 3.1 it was proven that when all initial values $\gamma_{i,j}(0)$ in the population of agents are nonzero, then at most $1 + 1/\sqrt{\beta_{ij}}$ clusters can be formed in the model with threshold $\tau=\sqrt{\beta_{ij}}$. The minimal distance between two clusters is $\sqrt{\beta_{ij}}$. In this section we investigate how parameters α_{ij} and β_{ij} influence the number and size of the clusters emerging in the scale-free and random networks. Furthermore, the rate of convergence of the agent opinions is determined for different parameter settings.

In the simulation study three values for β_{ij}: 0.001, 0.0025, 0.01 and three values for α_{ij}: 1, 10, 20 were used. According to the findings from Section 3.1, at most 33 clusters could emerge for β_{ij}=0.001, 21 clusters for β_{ij}=0.0025 and 11 clusters for β_{ij}=0.01 (see Fig. 1 for some examples of the simulation results).

In the networks used in the simulation less clusters were formed, as these networks were not fully connected. For $\beta_{ij} > 0.01$, in most cases only one cluster was formed containing all the agents. The minimal distances between the clusters in the simulated networks were greater than $\sqrt{\beta_{ij}}$. (Table 1).

In the tables with the results small clusters have the size up to 101 agents; medium clusters contain more than 100 but less than 1001 agents, and large clusters comprise of more than 1000 agents.

Besides β_{ij}, parameter α_{ij} also influences the number of clusters with the limit $1 + 1/\sqrt{\beta_{ij}}$ (Tables 2, 3), however in a more intricate manner. For example, in the random networks the largest number of clusters emerges when α_{ij} takes intermediate values (around 10), whereas in the scale-free networks many clusters tend to form with low values of α_{ij}.

In the random networks simulated with *M1* model only small and large size clusters tend to form (Table 4). Only one large size cluster emerges in the *M1*-based simulations, which contains the great majority of the agents in the population. Model *M2* produces also medium size clusters, but their amount is less than the number of the small size clusters. This can be partially explained by the absence of central agents or hubs with many connections in the random networks. Such agents would be able to attract large groups of other agents and influence their opinions so that the whole agent population may become polarized in larger opposing clusters. More medium size clusters tend to emerge in the scale-free networks simulated with both *M1* and *M2* models (Tables 3 and 5). The scale-free network topology contains hub agents. When such agents have opposing opinions, they form the basis for future clusters in which the whole population is divided. Because of such agents, who group others around themselves, the small and medium size clusters in the scale-free networks are on average larger than the ones emerging in the random networks (Tables 4 and 5). According to the analytical results from Section 3.1, the links between the agents within a cluster in model *M1* become stronger and the corresponding degrees of influence $\gamma_{i,j}(t)$ gradually tend to *1*, whereas the links between the agents from different clusters gradually disappear. In contrast to *M1*, links in *M2* appear and disappear instantaneously, depending on the states of the agents, which leads to faster and more abrupt cluster formation. Intuitively, this may be compared to instantaneous decision making (e.g., under high stress) without more detailed consideration and discussion. Because of this, in *M2* agents break links more easily than in *M1*, and thus, more clusters emerge (Tables 2, 3).

Based on the analytical and simulation results described in this section, model abstraction techniques are proposed in the following section 4.

Table 1. The minimal distances between the clusters in 10 random and 10 scale-free networks determined by simulation and analytically

Parameter settings	β=0.001			β=0.0025			β=0.01		
	α=1	α=10	α=20	α=1	α=10	α=20	α=1	α=10	α=20
Scale-free	0.034	0.041	0.038	0.053	0.059	0.07	1 cluster		
Random	0.041	0.034	0.033	0.1	0.084	0.2	0.4	0.15	0.23
Analytical	0.032			0.05			0.1		

Table 2. The mean and standard deviation values (in parentheses) of the numbers of small (≤ 100 agents), medium (>100 and ≤ 1000 agents) and large (>1000 agents) size clusters emerging in 10 random networks

Parameter settings	β=0.001			β=0.0025			β=0.01		
	α=1	α=10	α=20	α=1	α=10	α=20	α=1	α=10	α=20
Small *M1*	1.1 (1)	4 (1.2)	2.9 (1.2)	0.6 (0.9)	1.9 (0.7)	1 (0.8)	0.2 (0.4)	0.3 (0.6)	0.2 (0.4)
Small *M2*	5.1 (1.1)			2.9 (0.9)			0.6 (0.5)		
Medium *M1*	0	0	0	0	0	0	0	0	0
Medium *M2*	3.8 (0.9)			2 (0.8)			0		
Large *M1*	1	1	1.1	1	1	1	1	1	1
Large *M2*	2.3 (0.6)			1.3 (0.5)			1		

Table 3. The mean and standard deviation values (in parentheses) of the numbers of small (≤ 100 agents), medium (>100 and ≤ 1000 agents) and large (>1000 agents) size clusters emerging in 10 scale-free networks

Parameter settings	β=0.001			β=0.0025			β=0.01		
	α=1	α=10	α=20	α=1	α=10	α=20	α=1	α=10	α=20
Small *M1*	5.9 (0.9)	2.4 (0.8)	0.6 (0.6)	1.8 (0.9)	0.8 (0.7)	0.1 (0.3)	0	0	0
Small *M2*	3.1 (1.3)			1.6 (0.8)			0.1 (0.3)		
Medium *M1*	0	2.4 (0.8)	2.8 (0.6)	0	1.6 (0.5)	1.6 (0.7)	0	0	0
Medium *M2*	6.6 (1.3)			4.1 (1)			1.6 (0.5)		
Large *M1*	1	1	1	1	1.1 (0.3)	1.2 (0.4)	1	1	1
Large *M2*	1.6 (0.5)			1.5 (0.5)			1		

Table 4. The mean and standard deviation values (in parentheses) of the sizes of small (≤ 100 agents), medium (>100 and ≤ 1000 agents) and large (>1000 agents) clusters emerging in 10 random networks

Parameter settings	β=0.001			β=0.0025			β=0.01		
	α=1	α=10	α=20	α=1	α=10	α=20	α=1	α=10	α=20
Small *M1*	1.1 (0.3)	2.2 (1.6)	2.1 (1.9)	1	1.7 (1.2)	1.6 (0.8)	1	1.3 (0.6)	1
Small *M2*	17.5 (22.1)			19.4 (25.2)			5.7 (3.4)		
Medium *M1*	0	0	0	0	0	0	0	0	0
Medium *M2*	405.7 (253.8)			439.7 (271.8)			0		
Large *M1*	4998 (1)	4996 (3)	4539 (1026)	4999 (1)	4997 (2)	4998 (1)	4999 (0.4)	4999 (1)	4998 (0.4)
Large *M2*	1465 (427)			3126 (1280)			4997 (3)		

Table 5. The mean and standard deviation values (in parentheses) of the sizes of small (≤ 100 agents), medium (>100 and ≤ 1000 agents) and large (>1000 agents) clusters emerging in 10 scale-free networks

Parameter settings	β=0.001			β=0.0025			β=0.01		
	α=1	α=10	α=20	α=1	α=10	α=20	α=1	α=10	α=20
Small *M1*	1.7 (0.9)	47.5 (35.9)	1	1.7 (0.7)	53.3 (34.6)	1	0	0	0
Small *M2*	30.4 (30)			36.7 (33)			48		
Medium *M1*	0	222 (136)	429 (166)	0	276 (173)	450 (192)	0	0	0
Medium *M2*	424.8 (242)			462.6 (271)			543.5 (241)		
Large *M1*	4990 (3)	4351 (228)	3797 (246)	4997 (1.8)	4105 (1051)	3566 (1200)	5000	5000	5000
Large *M2*	1314 (165)			2030 (727)			4126 (131)		

4 Model Abstraction

In the model introduced in Section 2, after some time, each group of agents in an emerging cluster can be considered as a single entity. This forms a basis for abstraction of the agent-based model into a population-based model. Such an abstraction process can be performed in two steps:

Step 1: Identification of clusters of agents.
Step 2: Approximation of the equilibrium opinion states of the identified clusters.

First, in section 4.1 step 1 is considered. Then, in section 4.2 step 2 is described.

4.1 Identification of Clusters

To identify clusters of agents, it needs to be determined, which degrees of influence of the agents tend to *1* and which ones tend to *0*. After that, a standard algorithm for identification of connected components in a graph (e.g., based on breadth-first or depth-first search) can be applied to isolate the clusters.

The prediction of the values of the degrees of influence is based on observations made in Section 2 concerning $\gamma_{i,j}(t)$ with $\gamma_{i,j}(0) > 0$:

- if agents *i* and *j* belong to the same cluster, then
  $lim_{t\to\infty} \gamma_{i,j}(t)=1$ and $lim_{t\to\infty} \gamma_{j,i}(t)=1$
- if agents *i* and *j* belong to different clusters, then
  $lim_{t\to\infty} \gamma_{i,j}(t)=0$ and $lim_{t\to\infty} \gamma_{j,i}(t)=0$

Furthermore, it was observed that $\gamma_{i,j}(t)$ tending to *0* are often monotonically nonincreasing, whereas $\gamma_{i,j}(t)$ tending to *1* often first decrease and then grow rapidly. As the dynamics of decision making produced by the model is highly non-linear and erratic, it is not feasible to make early analytical predictions for the values of the degrees of influence. A heuristic approach is used instead.

The approach is based on identifying in each simulation the earliest time point after which it could be predicted with a high confidence whether each $\gamma_{i,j}(t)$ with $\gamma_{i,j}(0) > 0$ tends to *1* or to *0*. This time point is estimated by performing numerous simulations and determining the earliest time points $tp_{i,j}$ for every $\gamma_{i,j}(t)$ after which the degrees of influence tending to *0* are nonincreasing and the degrees of influence tending to *1* are nondecreasing, formally:

For $\gamma_{i,j}(t)\to 0$: $\{tp_{i,j} | \exists t1,t2\ t2 > t1 \,\&\, t1 \geq tp_{i,j} \,\&\, \gamma_{i,j}(t2) \leq \gamma_{i,j}(t1)$
$\&\ (tp_{i,j}=0 \,||\, tp_{i,j}>0 \,\&\, \gamma_{i,j}(tp_{i,j}) > \gamma_{i,j}(tp_{i,j}-\Delta t))\}$

For $\gamma_{i,j}(t)\to 1$: $\{tp_{i,j} | \exists t1,t2\ t2 > t1 \,\&\, t1 \geq tp_{i,j} \,\&\, \gamma_{i,j}(t2) \geq \gamma_{i,j}(t1)$
$\&\ (tp_{i,j} = 0 \,||\, tp_{i,j}>0 \,\&\, \gamma_{i,j}(tp_{i,j}) < \gamma_{i,j}(tp_{i,j}-\Delta t))\}$

In Table 6 the distribution (in %) of time points $tp_{i,j}$ in time intervals is provided, which is obtained by performing 1000 simulation for each setting of the model from Section 2. In each simulation a new network was generated with the uniformly distributed parameters: $\beta_{ij} \in [0.001, 0.09]$ and $\alpha_{ij} \in [1, 20]$. For the justification of the choice for the parameter ranges we refer to [11].

The values to the left and right from symbol 'l' in each data cell in the table indicate correspondingly the percentage of time points $tp_{i,j}$ for the degrees of influence tending to *1* and the percentage of time points $tp_{i,j}$ for the degrees of influence tending to *0*.

As can be seen from the table, starting already from time point 5 more than *95%* of the degrees of influence of the agents were either nonincreasing (in case of $\gamma_{i,j}(t)\to 0$) or nondecreasing (in case of $\gamma_{i,j}(t)\to 1$). The number of agents does not influence the distribution of $tp_{i,j}$ substantially. According to the obtained results, the degrees of influence tending to *0* become nonincreasing on average earlier (at time point 35 at

latest) than the degrees of influence tending to *1* become nondecreasing (this may even occur after time point 65). This is also in accordance with the simulation results discussed in Section 2: the degrees of influence tending to *0* grow rarely after the initial stabilization period (up to time point 15). Based on the obtained simulation results the following heuristic rules for determining the limit values of the degrees of influence ($\gamma_{i,j}$*) are specified:

Rule 1: If at control point t

$(\gamma_{i,j}(t) - \gamma_{i,j}(t-\Delta t))/\Delta t \geq 0$ and $\gamma_{i,j}(t) > 0.5$, Then $\gamma_{i,j}^* = 1$

Rule 2: If at control point t

$(\gamma_{i,j}(t) - \gamma_{i,j}(t-\Delta t))/\Delta t < 0$ and $\gamma_{i,j}(t) < 0.1$, Then $\gamma_{i,j}^* = 0$

Table 6. The distribution (in %) in time intervals of the earliest time points after which the degrees of influence tending to *0* are nonincreasing and the degrees of influence tending to *1* are nondecreasing; the results are based on 1000 simulation trials

Setting Time interval	100 agents, scale free	1000 agents, scale free	100 agents, random	1000 agents, random
[0, 5]	96.7 | 100	96.7 | 98.5	95.7 | 100	95.4 | 100
(5, 15]	2.71 | 0	2.6 | 1.12	3.2 | 0	3.43 | 0
(15, 25]	0.29 | 0	0.33 | 0	0.5 | 0	0.5 | 0
(25, 35]	0.13 | 0	0.13 | 0.13	0.15 | 0	0.19 | 0
(35, 45]	0.07 | 0	0.07 | 0	0.09 | 0	0.1 | 0
(45, 55]	0.05 | 0	0.04 | 0	0.07 | 0	0.07 | 0
(55, 65]	0.03 | 0	0.004 | 0	0.05 | 0	0.04 | 0
> 65	0.07 | 0	0.11 | 0	0.24 | 0	0.27 | 0

The first control time point is set at 5, as according to Table 6 for more than 95% of the degrees of influence the correct prediction for the limit values could have been made at this point. The last control point is set at 65, and the distance between two control points is 10. The constraints $\gamma_{i,j}(t) > 0.5$ and $\gamma_{i,j}(t) < 0.1$ were identified statistically using the obtained simulation results by determining minimum (maximum) $\gamma_{i,j}(t)$ values for the degrees of influence tending to *1* (to *0*) at the control points.

Based on the identified heuristic rules the algorithm below is defined. At each control point the number of limit values $\gamma_{i,j}$* is counted (variable *count*) that can be initialized according to the rules above (lines 4-16). If this number exceeds *90%* of all $\gamma_{i,j}$ with $\gamma_{i,j}(0) > 0$, the algorithm terminates and the identification of clusters (i.e., connected components in a graph) starts (lines 17,18). Otherwise, the algorithm proceeds with checking for the following control time point. Thus, the time point when clustering starts varies between simulations; it depends on the parameter and initial value settings of the model. Note that for those $\gamma_{i,j}$ for which the heuristic rules do not hold, weaker versions of the rules are applied without constraints $\gamma_{i,j}(t) > 0.5$ and $\gamma_{i,j}(t) < 0.1$. The obtained $\gamma_{i,j}$* are not taken into account in variable *count*, as they are considered to be unreliable. After the algorithm terminates, automated clustering is performed by breadth-first search.

The algorithms for determining limit values and clustering were implemented in Matlab. Again, 1000 simulations were performed for each setting from Table 6 and

the number of agents was determined that were assigned to a wrong cluster; the errors (in % of agents) averaged over all simulation trials for each simulation setting are provided in Fig. 2. It is important to know the characteristic behaviour of the clustering error to determine the time point when the model abstraction should be done. On the one hand, if the model abstraction is done too late, the computational gain obtained by the abstraction may be low. On the other hand, if the model abstraction is done too early, the approximation error of the obtained abstracted model may be high.

Algorithm 1. Determining limit values for the degrees of influence

```
1: m_count ← ( the number of γ_{i,j}(0) > 0)
2: for t=5 to 65 step 10 do
3:     count ← 0
4:     for all agents i, j do
5:       if γ_{i,j}(0)>0
6:          if (γ_{i,j}(t)- γ_{i,j}(t-Δt))/Δt ≥0
7:              γ_{i,j}* ← 1
8:              if γ_{i,j}(t) > 0.5
9:                  count ← count+1 endif
10:         else if (γ_{i,j}(t)- γ_{i,j}(t-Δt))/Δt < 0
11:             γ_{i,j}* ← 0
12:             if γ_{i,j}(t) < 0.1
13:                 count ← count+1 endif
14:       endif
15:     endif
16:   end for
17:   if count > 0.9* m_count
18:       start clustering; exit  endif
19: end for
20: start clustering
```

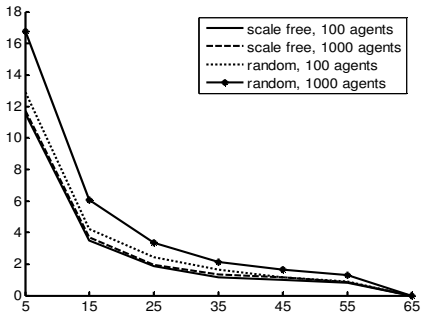

Fig. 2. The percentage of agents assigned to wrong clusters in all simulation settings. The horizontal axis is time and the vertical axis is the % of agents from the whole population.

The clustering error of the scale-free networks is in average lower than the error of the random networks (Fig. 2). This can partially be explained by a higher convergence rate of the scale-free networks observed in the study. Furthermore, in contrast to the random networks, the clustering error of the scale-free networks does not depend significantly on the number of agents.

After the agents have been divided into clusters, the values of the opinion states of the clusters are determined, which is step 2 of the abstraction procedure discussed in the following section 4.2.

4.2 Approximation of States of the Clusters

For the approximation of the states of each cluster the abstraction method based on invariant calculation from [10] is used. This method demonstrated the best precision and computational efficiency in comparison with other methods. In our abstraction procedure this method is applied for each cluster separately at the time point, when

clustering of agents is performed. A concise summary of the invariant-based abstraction method is provided below. For more details please refer to [10].

For given initial values $q_{s,i}(0)$ for $i = 1, ..,$ only one of the possible equilibria with equal values will be actually reached. How this equilibrium value depends on the initial values can be described by an *invariant*: an expression in terms of the $q_{s,i}(t)$ for $i = 1, ..,$ that does not change over time. In this case an invariant inv_s as a weighted sum $inv_s = inv_s(t) = \sum_i \lambda_{s,i} q_{s,i}(t)$ can be obtained where the weights $\lambda_{s,i}$ depend on the coefficients η_i and $\gamma_{j,i}$ (and not on initial values). These weights can be taken (normalised) with $\sum_i \lambda_{s,i} = 1$, so that when all $q_{s,i}(t) = 1$ for all i, also the invariant is 1. Below it will be discussed how an invariant can be found.

An invariant can be considered as a kind of preservation law for the (collective) support for option s in the considered group. By internal (intragroup) interactions this collective support for s can be redistributed over persons in the group, but this does not change the collective amount. During time intervals where no external interaction is coming in, the group's collective support for s will not change. This provides an interesting use of the invariant: as a means of abstraction from the internal processes by using a descriptor at the group level.

The weights $\lambda_{s,i}$ for the invariant inv_s can be determined from the difference equations:

$$\sum_m \sum_{i \neq m} \lambda_{s,i} \eta_i \gamma_{m,i} q_{s,m}(t) = \sum_m \lambda_{s,m} \eta_m q_{s,m}(t)$$

One way to satisfy this is by taking the coefficients of $q_{s,m}(t)$ in the above expression on both sides equal; this provides the following set of linear equations for the $\lambda_{s,i}$ for all m:

$$\sum_{i \neq m} (\eta_i \gamma_{m,i} / \eta_m) + 1) \lambda_{s,i} = 1$$

Thus a system of linear equations $\sum_{i \neq m} \mu_{m.i} \lambda_{s,i} = 1$ is found with coefficients $\mu_{m.i} = (\eta_i \gamma_{m,i} / \eta_m) + 1 \geq 1$.

This system can be described in matrix form as $\mathbf{A}\boldsymbol{\lambda}_s = \mathbf{1}$, where $\mathbf{1}$ is the vector with all components 1, $\boldsymbol{\lambda}_s = (\lambda_{s,1},\ldots)$, and $\mathbf{A}$ is a square matrix with only zeros at the diagonal and all other entries ≥ 1 (expressed in η_i and $\gamma_{m,i}$). When it is assumed that the determinant $\mathbf{det(A)} \neq 0$, then this system has a unique solution. Indeed, for the general case this condition is fulfilled, and the weights $\lambda_{s,i}$ of the invariant can be obtained as a solution.

To illustrate the abstraction procedure, 1000 simulations were performed. In each simulation a new network was generated. In each simulation clusters of agents were identified using the approach from Section 3.1. Then, the invariant-based method was applied to approximate the limit values of the opinion states of the clusters. The averaged approximation error per agent for each simulation was defined as:

$$err = \sum_{i \in AGENT} |q^*_{s,i} - q_{s,i}(end\_time)| / |AGENT|,$$

where *AGENT* is the set of all agents, *end_time* is the simulation time, $q^*_{s,i}$ is the predicted opinion state value for option s of the cluster, to which agent i belongs; it is determined by the invariant-based abstraction.

Furthermore, the time was measured for each simulation and the simulation efficiency gain was determined as the ratio of the simulation time of the model with

abstraction to the simulation time of the original model without abstraction. In the model with abstraction the clusters of agents were replaced by single super-agents with the cluster states determined by the proposed abstraction approach.

The obtained results averaged over 1000 simulations are provided in Table 7. As can be seen from the table, the number of agents influences more significantly the approximation error in the random networks than in the scale-free networks. As was shown in [11], agent states propagate slowly through a random network with a low average node degree. The simulation showed that with the increase of the number of agents, the state propagation speed and the convergence speed of such networks decreases. This causes an increase of the error of the equilibrium-based abstraction employed in the paper.

Table 7. The approximation error and the efficiency gain of the abstracted model evaluated for the simulation settings. The values in brackets for the approximation error are variances.

Setting / **Result**	***100 agents, scale free***	***1000 agents, scale free***	***100 agents, random***	***1000 agents, random***
Approx. error (err)	$13*10^{-4}$ ($2*10^{-4}$)	$14*10^{-4}$ ($3*10^{-4}$)	$27*10^{-4}$ ($3*10^{-4}$)	$159*10^{-4}$ ($5*10^{-4}$)
Simulation time, s	1.42	5.12	1.45	5.19
Efficiency gain	5.7	6	6.2	6

Furthermore, the approximation error is lower for the scale-free networks than for the random networks. This could also be partially explained by the difference in the network convergence speeds: the scale-free networks reach an equilibrium state faster than the random networks, and thus the equilibrium-based abstraction is more precise for the scale-free networks. The simulation efficiency gain is approximately the same (around 6) for both network types and for different numbers of agents.

Note that the values of the states for the clusters were determined at the same time point in interval [5, 65], when the clustering was performed. At this time point some degrees of influence may not have reached equilibrium yet. Thus, weak connections between clusters might still have existed, contributing to the approximation error. This issue may partially be addressed by considering clusters as aggregated agents interacting with each other, as was done in [10]. However, for some networks such interactions may be numerous, and thus would have a large negative effect on the computational efficiency. A precise performance analysis for such an aggregated form of modelling is not considered in this paper and will be addressed in the future.

5 Discussion

In the paper simulation results were presented for the networks with the average node degree 4.5. However, also experiments for more dense networks were performed. In general, the higher the density of a network, the higher its asymptotic convergence speed to an equilibrium state and the less number of clusters are formed. Furthermore, in average the higher the density of the network, the less the approximation error by the equilibrium-based abstraction.

Besides the parallel mode of interaction we also performed simulation for the sequential interaction mode. In the latter mode two randomly chosen agents interacted in each iteration. Small, medium and large clusters emerged in this case as well, however their numbers were lower than in the parallel case, and the asymptotic convergence speed was higher.

Simulations were also performed for model variants, in which agents exchanged opinions on multiple topics at the same time. For these models two alternatives exist: 1) to introduce a separate degree of influence for each topic, or 2) to use one degree of influence for all topics. Also clusters can be considered for each topic separately or by introducing a similarity measure of the agents combining all the topics (e.g., based on the Euclidean distance). In all these cases small, medium and large clusters emerged. However, the asymptotic convergence speed was significantly slower than in the case with one topic.

Several techniques for abstraction of models based on hybrid automata and differential equations [18] currently exist. However, such approaches can be efficiently applied for systems described by sparse matrixes. Social contagion models represent tightly connected systems, which do not allow a significant reduction of the state space using such techniques. In particular, a previous study showed that common model reduction techniques such as balanced truncation [18] do not allow decreasing the rank of the matrix describing the model from Section 2. In [17] abstraction of social contagion models with static networks is considered. However, the emergent behaviour of social contagion models with static networks is very different from the behaviour of models with dynamic networks (e.g., no emergence of clusters in static networks). Thus, the abstraction approach proposed in this paper differs substantially from the approach taken in [17].

6 Conclusions

In this paper an agent-based social decision making model based on social contagion with a dynamic network is proposed. In contrast to the existing models [2, 4, 7, 8], similarity in agent states or opinions has a dynamic effect on the strengths of the links between agents: they change gradually over time, rather than that a more static effect is used based on a threshold mechanism. The model was analysed analytically and by simulation. Cluster formation has been extensively investigated in the paper for the models with gradually and abruptly changing links: the distribution of clusters in random and scale-free networks was investigated, the dynamics of links within and between clusters were determined, the minimal distance between two clusters was identified.

Furthermore, in the paper an approach for abstraction of social contagion models with underlying dynamic networks is proposed. On the one hand, it enables analysis of emergent properties of a model by approximating with a high accuracy its global dynamics at the population level. On the other hand, the approach increases the computational efficiency of agent-based simulations of social contagion models (6 times for the model considered in the paper).

Acknowledgement

One of the authors was supported by the Dutch Technology Foundation STW, which is the applied science division of NWO, and the Technology Program of the Ministry of Economic Affairs.

References

[1] R. Axelrod. The Dissemination of Culture: A Model with Local Convergence and Global Polarization. Journal of Conflict Resolution 41: 2023-226, 1997.
[2] V.D. Blondel, J. M. Hendrickx, and J.N. Tsitsiklis. On Krause's consensus formation model with state-dependent connectivity. IEEE Trans. on Automatic Control, vol. 54(11), pp. 2506-2517, 2009.
[3] D. Byrne, The attraction hypothesis: Do similar attitudes affect anything? Journal of Personality and Social Psychology, 51(6), 1986, 1167-1170.
[4] G. Deffuant, D. Neau, F. Amblard, and G.Weisbuch. Mixing beliefs among interacting agents. Adv Complex Syst, 3. pp. 87-98, 2000.
[5] J.R., French. A Formal Theory of Social Power. Irvington Publishers, 1993.
[6] J. Golbeck. Computing and Applying Trust in Web-based Social Networks. PhD Thesis, University of Maryland, 2005.
[7] M. Granovetter. Threshold Models of Collective Behavior. American Journal of Sociology, 83(6):1420:1443, 1978.
[8] R. Hegselmann and U. Krause. Opinion dynamics and bounded confidence: models, analysis and simulation, J.of Artificial Societies and Social Simulation 5, 3, 2002.
[9] M. Hoogendoorn, J. Treur, C.N. van der Wal, and A. van Wissen. An Agent-Based Model for the Interplay of Information and Emotion in Social Diffusion. In Proceedings of IAT'10. IEEE Computer Society Press, 439-444, 2010.
[10] K. Lewin. Group Decision and Social Change. New York: Holt and Winston, 1958.
[11] M. McPherson, L. Smith-Lovin, J. M. Cook (2001). Birds of a feather: homophily in social networks. Annu. Rev. Sociol. 27, 415–444 (2001).
[12] M. Macy, J. A. Kitts, and A. Flache. Polarization in Dynamic Networks: A Hopfield Model of Emergent Structure. In Dynamic Social Network Modeling and Analysis. Washington, DC: National Academies Press, 162-173, 2003.
[13] L. Muchnik, R. Itzhack, S. Solomon, and Y. Louzoun, Self-emergence of knowledge trees: Extraction of the Wikipedia hierarchies, Phys. Rev. E 76, 016106 (2007)
[14] H.V.D. Parunak, T.C. Belding, R. Hilscher, and S. Brueckner. Modeling and Managing Collective Cognitive Convergence. In Proceedings of AAMAS 2008, pp. 1505-1508, ACM Press, 2008.
[15] O. Reingold. Undirected connectivity in log-space. Journal of the ACM 55 (4), pp. 17- 24, 2008
[16] A. Sharpanskykh. Managing the Complexity of Large-Scale Agent-based Social Diffusion Models with Different Network Topologies. In Proceedings of the 12th Pacific Rim International Conference on Artificial Intelligence (PRICAI'12), Springer Verlag, Lecture Notes in Computer Science, Vol. 7458, 2012, pp. 540-551.
[17] A. Sharpanskykh, J. Treur. Group Abstraction for Large-Scale Agent-Based Social Diffusion Models. In: Zhan, J., et al. (eds.), Proceedings of the Third International Conference on Social Computing, SocialCom'11. IEEE Computer Society Press, 2011, pp.830-837.

[18] A.C. Antoulas and D. C. Sorensen. Approximation of large-scale dynamical systems: An overview. Int. J. Appl. Math. Comp. Sci., 11:1093-1121, 2001.